

Self-consistent tensor network method for correlated super-moiré matter beyond one billion sites

Yitao Sun,¹ Marcel Niedermeier,¹ Tiago V. C. Antão,¹ Adolfo O. Fumega,¹ and Jose L. Lado¹

¹*Department of Applied Physics, Aalto University, 02150 Espoo, Finland*

(Dated: March 7, 2025)

Moiré and super-moiré materials provide exceptional platforms to engineer exotic correlated quantum matter. The vast number of sites required to model moiré systems in real space remains a formidable challenge due to the immense computational resources required. Super-moiré materials push this requirement to the limit, where millions or even billions of sites need to be considered, a requirement beyond the capabilities of conventional methods for interacting systems. Here, we establish a methodology that allows solving correlated states in systems reaching a billion sites, that exploits tensor-network representations of real-space Hamiltonians and self-consistent real-space mean-field equations. Our method combines a tensor-network kernel polynomial method with quantics tensor cross interpolation algorithm, enabling us to solve exponentially large models, including those whose single particle Hamiltonian is too large to be stored explicitly. We demonstrate our methodology with super-moiré systems featuring spatially modulated hoppings, many-body interactions and domain walls, showing that it allows access to self-consistent symmetry broken states and spectral functions of real-space models reaching a billion sites. Our methodology provides a strategy to solve exceptionally large interacting problems, providing a widely applicable strategy to compute correlated super-moiré quantum matter.

Introduction—Twisted moiré materials have enabled creating of a wide variety of correlated states of matter, including unconventional superconducting phases [1–6], topological states [7–10] and correlated insulators [11–14]. These emergent states stem from the moiré pattern between twisted or mismatched 2D materials [15], ideas that have been extended to a variety of artificial platform including optical metamaterials [16–22] and cold atom systems [23–26]. The moiré pattern gives rise to an emergent periodicity and associated unit cells ranging from thousands to hundreds of thousands of sites, reaching the limits of theoretical atomistic methods to study correlated phases [27–30]. When two or more moiré patterns coexist, a super-moiré emerges, leading to an even wider variety of exotic phases [31, 32]. However, super-moiré materials require treating systems from millions to hundreds of millions of sites, which is a challenge for conventional computational methods.

In many-body physics, tensor network algorithms have provided an exceptional method to treat systems with exponentially large many-body Hilbert spaces [33–36]. The essence of tensor networks is to compress an exponentially large Hilbert space of dimension 2^L with a linearly scaling variational product of tensors. This strategy has provided the most accurate solutions to paradigmatic quantum many-body problems, and has been recently extended to tackle problems in machine learning [37–39], quantum chemistry [40–42], quantum computing [43–45], quantum error correction [46–48] and ultimately general problems that require dealing with exponentially large structures of data and integrals [49–55]. Therefore, the capability of tensor networks to deal with exponentially large systems may provide a way forward to tackle problems of interacting super-moiré materials [56].

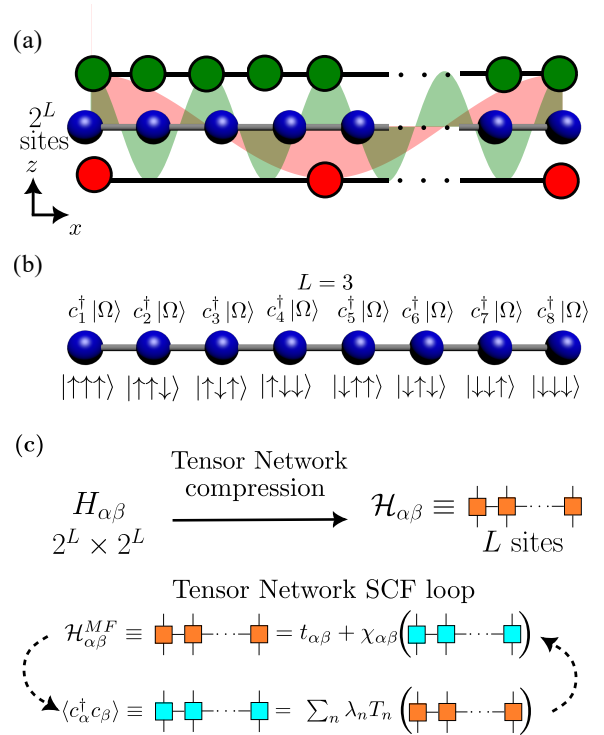


FIG. 1. Panel (a) shows a schematic of a system featuring two moiré patterns due to the mismatch of a top and bottom substrate. Panel (b) shows an example for representing electron states in fermionic and pseudo-spin basis. Panel (c) shows the tensor-network compression and mean-field algorithm, where the exponentially large fermionic problem is mapped to a linearly scaling pseudo-spin problem.

In this letter, we establish a tensor network methodology to solve correlated states in super-moiré systems reaching a billion sites. Our method uses an atomistic

self-consistent mean-field approach where both single particle and interacting mean-field terms are expressed purely as tensor networks, using a combination of tensor-network Chebyshev expansions and quantum cross interpolation. Our strategy leverages a mapping between the mean-field Hamiltonian of an exponentially large super-moiré system to a linearly scaling pseudo-spin many-body problem. This methodology allows for the treatment of super-moiré systems whose mean-field Hamiltonian is too large to be explicitly stored, enabling dealing with system sizes beyond the capabilities of techniques with sparse matrix representations. We demonstrate our method in super-moiré structures with over one billion atomic sites, showing that it allows us to solve self-consistently interacting problems with spatially varying hoppings and interactions. This work thus provides a methodology capable of dealing with the exceptional system sizes required for correlated phases in super-moiré quantum matter.

Self-consistent tensor network algorithm—We consider a generic interacting real-space Hamiltonian of a super-moiré system with $N = 2^L$ sites as shown in Fig. 1 (a), that has both single particle and density-density many-body interaction taking the form

$$H = H_0 + H_V = \sum_{\alpha\beta} t_{\alpha\beta} c_{\alpha}^{\dagger} c_{\beta} + \sum_{\alpha\beta} V_{\alpha\beta} c_{\alpha}^{\dagger} c_{\alpha} c_{\beta}^{\dagger} c_{\beta}, \quad (1)$$

where $t_{\alpha\beta}$ are single-particle hopping amplitudes in the system and $V_{\alpha\beta}$ account for the many-body density-density interactions. The previous Hamiltonian can be solved at the mean-field level by performing the mean-field decoupling $H_V \approx H_V^{MF}$ where $H_V^{MF} = \sum_{\alpha\beta} V_{\alpha\beta} \langle c_{\alpha}^{\dagger} c_{\alpha} \rangle c_{\beta}^{\dagger} c_{\beta} + \dots = \sum_{\alpha\beta} \chi_{\alpha\beta} c_{\alpha}^{\dagger} c_{\beta}$, \dots denoting the remaining Wick contractions. This decoupling gives rise to a mean-field Hamiltonian of the form

$$H^{MF} = \sum_{\alpha\beta} (t_{\alpha\beta} + \chi_{\alpha\beta}) c_{\alpha}^{\dagger} c_{\beta} = \sum_{\alpha\beta} H_{\alpha\beta}^{MF} c_{\alpha}^{\dagger} c_{\beta}, \quad (2)$$

with $H_{\alpha\beta}^{MF} \equiv H_{\alpha\beta}^{MF} [V_{\alpha\beta}, \langle c_{\alpha}^{\dagger} c_{\beta} \rangle]$ parametrizes the self-consistent mean-field Hamiltonian including single-particle and many-body corrections. For exponentially large systems, the mean-field Hamiltonian H^{MF} becomes too large to be even stored. We can now reinterpret the 2^L -site mean-field Hamiltonian as a many-body operator of an auxiliary many-body pseudo-spin chain of L sites, for which the index α, β corresponds to an element of the pseudo-spin many-body basis as $\alpha \equiv (s_1, s_2, \dots, s_L)$ and $\beta \equiv (s'_1, s'_2, \dots, s'_L)$. In this form, the mean-field Hamiltonian can be written using a tensor-network representation as a matrix product operator (MPO) in the pseudo-spin basis as

$$\mathcal{H}_{\alpha\beta}^{MF} \equiv \Gamma_{s_1, s'_1}^{(1)} \Gamma_{s_2, s'_2}^{(2)} \Gamma_{s_3, s'_3}^{(3)} \dots \Gamma_{s_L, s'_L}^{(L)}, \quad (3)$$

where $\Gamma_{s_1, s'_1}^{(n)}$ are tensors of dimension m , the bond dimension of the MPO. The structured nature of a super-

moiré Hamiltonian enables the representation of $H_{\alpha\beta}^{MF}$ with a manageable bond dimension [49, 50]. The main problem to solve the interacting system is then to find the tensor-network representation \mathcal{H}^{MF} of H^{MF} in Eq. 2, which can be done by solving a Chebyshev tensor-network self-consistent equation [57–60]. The essential objects to compute are correlators $\langle c_{\alpha}^{\dagger} c_{\beta} \rangle = \int_{-\infty}^{\epsilon_F} \langle \alpha | \delta(\omega - \mathcal{H}^{MF}) | \beta \rangle d\omega$, with the matrix product state (MPS) $|\alpha\rangle = c_{\alpha}^{\dagger} |\Omega\rangle$ as shown in Fig. 1 (b), $|\Omega\rangle$ the vacuum state, ϵ_F the Fermi energy and $\delta(\omega - \mathcal{H}^{MF})$ Dirac delta function operator. We can now compute all the expectation values as

$$\langle c_{\alpha}^{\dagger} c_{\beta} \rangle = \langle \alpha | \Xi(\mathcal{H}^{MF}) | \beta \rangle, \quad (4)$$

where $\Xi(\mathcal{H}^{MF})$ is the tensor-network representation of the density matrix computed with a tensor-network Chebyshev kernel polynomial method (KPM) [61–64]. By rescaling the bandwidth of \mathcal{H}^{MF} to the interval $(-1, 1)$, the density matrix takes the form

$$\Xi(\mathcal{H}^{MF}) = \sum_n \lambda_n T_n(\mathcal{H}^{MF}), \quad (5)$$

where $T_n(x)$ are the Chebyshev polynomials with recursion relation $T_n(x) = 2xT_{n-1}(x) - T_{n-2}(x)$ with $T_0 = 1$ and $T_1 = x$ [65]. The expansion coefficients are $\lambda_n = \int_{-1}^{\epsilon_F} \frac{2T_n(\omega)}{\pi\sqrt{1-\omega^2}} d\omega$ for $n \geq 1$ and $\lambda_0 = \int_{-1}^{\epsilon_F} \frac{T_0(\omega)}{\pi\sqrt{1-\omega^2}} d\omega$. These Chebyshev recursion relations allow us to find a tensor-network representation of Eq. 5 by performing sums and contractions between MPOs. While Eq. 5 is not of practical use with large sparse matrix representations, it can be directly applied with MPO [66].

The previous Chebyshev expansion gives access to all the correlators $\langle c_{\alpha}^{\dagger} c_{\beta} \rangle$. The mean-field decoupling allows us to define a new mean-field Hamiltonian from the tensor-network representation of the correlators combining Eq. 4, Eq. 5 and Eq. 2 as shown in Fig. 1 (c). Once the self-consistent mean-field Hamiltonian has been obtained, the spatially dependent spectral function $D(\omega, \alpha) = \langle \alpha | \delta(\omega - \mathcal{H}^{MF}) | \alpha \rangle$ of the interacting problem can be computed using a tensor-network Chebyshev expansion as

$$D(\omega, \alpha) = \langle \alpha | \left[\sum_n T_n(\mathcal{H}^{MF}) P_n(\omega) \right] | \alpha \rangle, \quad (6)$$

where $P_n(\omega) = \frac{2T_n(\omega)}{\pi\sqrt{1-\omega^2}}$ for $n \geq 1$ and $P_0(\omega) = \frac{T_0(\omega)}{\pi\sqrt{1-\omega^2}}$.

Tensor-network representation of the super-moiré hopping and mean-field interactions—We now elaborate on the explicit form of the MPO representation of the single particle Hamiltonian H_0 . For concreteness, we will focus on a one-dimensional spinful Fermi-Hubbard type

Hamiltonian as

$$H = \sum_{\alpha,s} t_{\alpha,\alpha+1} c_{x_{\alpha+1},s}^\dagger c_{x_\alpha,s} + h.c. + \sum_{\alpha} U_{\alpha} \left(c_{x_{\alpha},\uparrow}^\dagger c_{x_{\alpha},\uparrow} - \frac{1}{2} \right) \left(c_{x_{\alpha},\downarrow}^\dagger c_{x_{\alpha},\downarrow} - \frac{1}{2} \right), \quad (7)$$

where $t_{\alpha,\alpha+1}$ captures the spatially varying hopping amplitude between two adjacent atomic sites x_α and $x_{\alpha+1}$ and U_α is the Hubbard interaction induced by the super-moiré correlation in a 1D moiré superlattice. We start with a 1D nearest neighbor hopping $H_{0,NN} = \sum_{\alpha,s} t(c_{x_{\alpha+1},s}^\dagger c_{x_\alpha,s} + h.c.)$, noting that this method can be extended to arbitrary range hopping. The MPO representation of the uniform $\mathcal{H}_{0,NN}$ hopping term takes the form [67] $\mathcal{H}_{0,NN} = \sum_{l,s} t(\sigma_{l,s}^+ \prod_{m>l} \sigma_{m,s}^- + h.c.)$, where $\sigma^\pm = \frac{1}{2}(\sigma_x \pm i\sigma_y)$, σ_x and σ_y being Pauli matrices. l and m are the site indices of the L -site MPO $\mathcal{H}_{0,NN}$. We then address the case of a spatially modulated hopping amplitude $t_{\alpha,\alpha+1} = t(X_\alpha)$, where $X_\alpha = \frac{x_\alpha + x_{\alpha+1}}{2}$. Viewing $t(X_\alpha)$ as a function of X_α , by applying the quantum tensor cross interpolation (QTCI) algorithm [49, 68, 69] over $t(X_\alpha)$ we now generate an MPS representation $|\tau\rangle = \sum M_{s_1}^{(1)} M_{s_2}^{(2)} M_{s_3}^{(3)} \dots M_{s_L}^{(L)} |s_1, s_2, \dots, s_L\rangle$ storing all $t(X_\alpha)$ values. For each $M_{s_j}^{(j)}$, we introduce an auxiliary index s'_j to obtain a new tensor $\Gamma_{s_j, s'_j}^{(j)}$ and enforce a diagonal matrix structure of the data encoded with a contraction of $\Gamma_{s_j, s'_j}^{(j)} \delta_{j,j'}$. Repeating this process for all tensors in $|\tau\rangle$ yields an MPO representation \mathcal{T} that stores a diagonal matrix whose elements are same as those of $|\tau\rangle$. Eventually we perform a contraction between \mathcal{T} and $\sum_{l,s} \sigma_{l,s}^+ \prod_{m>l} \sigma_{m,s}^-$, producing an MPO representation of the single electron Hamiltonian

$$\mathcal{H}_0 = \{[\mathcal{T} \sum_{l,s} (\sigma_{l,s}^+ \prod_{m>l} \sigma_{m,s}^-)] + h.c.\}. \quad (8)$$

The MPO \mathcal{H}_0 faithfully stores the original hopping terms, ensuring $\langle x_\alpha, s | \mathcal{H}_0 | x_{\alpha+1}, s \rangle \approx t(X_\alpha)$.

We can construct H_V in an analogous manner. Given an initial guess of $\langle c_{x_\alpha, s}^\dagger c_{x_\alpha, s} \rangle$ for spin- s electrons across the system, we can view it as a function of x_α . Utilizing the same approach used for \mathcal{H}_0 , we can construct an MPS $|\nu_s\rangle$ followed by its diagonal MPO representation \mathcal{N}_s storing the previous guess. The MPO representation of the interaction term reads $\mathcal{H}_{V,s} = U_\alpha \mathcal{N}_s$. This very same approach could be applied for spatially varying Hubbard interactions. As one can build an MPO representation \mathcal{U} similar to the building of \mathcal{T} , the interaction term will be a simple contraction $\mathcal{H}_{V,s} = \mathcal{U} \mathcal{N}_s$. The full interaction MPO \mathcal{H}_V will then be $\sum_s \mathcal{H}_{V,s}$.

Billion site interacting problem—We now show results for the one-dimensional model of Eq. 7, with length of $2^{30} (\gtrsim 10^9)$ atomic sites. Such a model can be realized

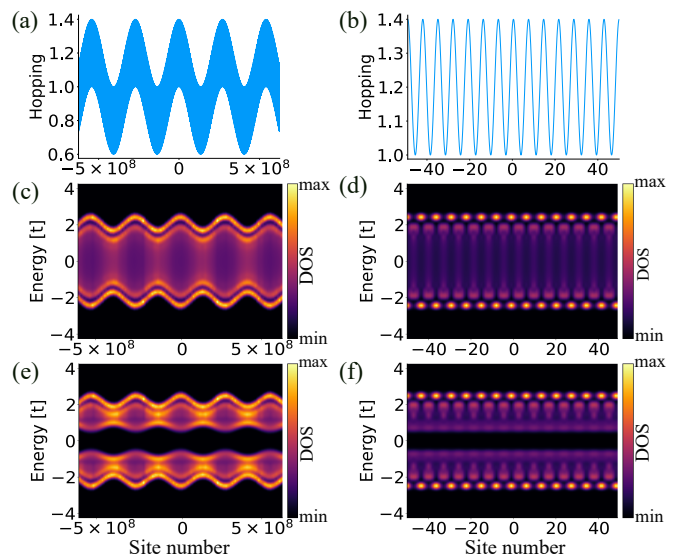


FIG. 2. Results for system with super-moiré modulation on hopping amplitudes. Panels (a) & (b) show the hopping amplitudes $t(X_\alpha)$ at the larger moiré scale and smaller moiré scale. Panels (c) & (d) show the corresponding local spectral functions calculated for system with $2^{30} \gtrsim 10^9$ sites without Hubbard interaction at 2 different moiré scales. Panels (e) & (f) show the corresponding local spectral functions calculated for system with Hubbard interaction at 2 different moiré scales.

using optical quantum simulation methods [16, 70] or in 1D multi-walled nanotubes [71]. We assume $t(X_\alpha)$ to have the form

$$t(X_\alpha) = t_0 + t_1 \cos(k_1 X_\alpha) + t_2 \cos(k_2 X_\alpha), \quad (9)$$

where we set $k_1 = \frac{2\pi}{5\sqrt{2}}$ and $k_2 = \frac{8\pi}{2^{29}\sqrt{3}}$. These correspond to two different moiré scales as shown in Fig. 2 (a) and Fig. 2 (b), which are incommensurate to each other throughout the system.

The local spectral functions for systems with and without Hubbard interaction are shown in Fig. 2 (c)-(f). All self-consistent field computations in this study were executed on a single core of an Intel i5 CPU. The calculation for the self-consistent solution is shown in Fig. 2 (e) and (f). This MPO-KPM-QTCI calculation featuring $2^{30} \gtrsim 10^9$ sites required a computational time of 4×10^4 seconds, leading to a speedup of around four orders of magnitude compared to the estimated time required with a sparse-KPM-QTCI method [56]. The interacting solution shows modulations of the spectral function following the larger moiré scale corresponding to k_2 and the smaller moiré scale corresponding to k_1 . In the presence of Hubbard on-site interactions, a spatially inhomogeneous gap emerges across the system, which exhibits spatial variations governed by the larger moiré scale yet remains nearly uniform at smaller moiré scale. This is due to the fact that the utilized scale of the Hubbard interaction is of the same order as the smaller moiré scale while

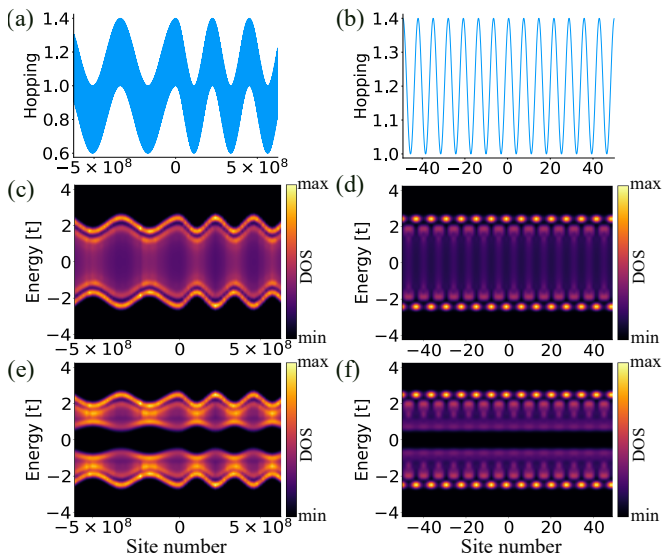


FIG. 3. Results for system with super-moiré modulation on hopping amplitudes with a domain wall in the middle of the system. Panels (a) & (b) show the hopping amplitudes $t(X_\alpha)$ with the domain wall and 2 different larger moiré scale and smaller moiré scale. Panels (c) & (d) show the corresponding local spectral functions calculated for system with $2^{30} \gtrsim 10^9$ sites without Hubbard interaction at 2 different moiré scales. Panels (e) & (f) show the corresponding local spectral functions calculated for system with Hubbard interaction at 2 different moiré scales.

being negligible in comparison to the larger moiré scale. Consequently, a uniform gap opens across all sites at the smaller moiré scale while being explicitly modulated by the super-moiré correlation at the larger moiré scale.

Another possibility is to consider similar systems with a super-moiré domain wall in the middle, which could happen due to the presence of strain or lattice relaxations in real physical systems [72–74]. We use the same form of Hamiltonian as in Eq. 7 but include the domain wall by modulating the larger moiré scale k_2 as

$$\tilde{k}_2 = k_2 \left[1 + \delta \tanh\left(\frac{X_\alpha}{W}\right) \right], \quad (10)$$

where δ is a parameter used to quantify the mismatch between the two larger moiré scales separated by the domain wall, and W is the width of the domain wall. We set $\delta = 0.2$, $W = \frac{2^{30}}{40}$ and keep other parameters consistent with the calculation without the presence of the domain wall. In Fig. 3 (c) and (e), it is clear that the local spectral functions closely follow the modulation of larger moiré scale on both sides of the domain wall. The opening of the gap due to the Hubbard interaction shown in Fig. 3 (e) also obeys this modulation, while at the smaller moiré scale spectral functions are not influenced by the domain wall as shown in Fig. 3 (d) and (f).

We have also applied our approach for a system with a super-moiré modulated Hubbard interaction as can be

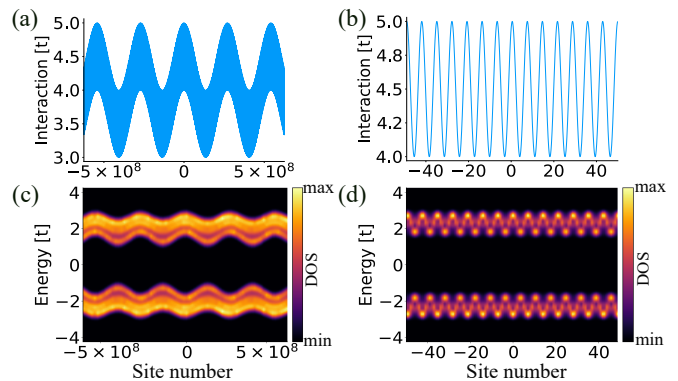


FIG. 4. Super-moiré Hubbard interaction. Panels (a) & (b) show the Hubbard interaction $U(x_\alpha)$ at the larger moiré scale and smaller moiré scale. Panels (c) & (d) show the corresponding local spectral functions calculated for system with $2^{30} \gtrsim 10^9$ sites at 2 different moiré scales.

realized through Coulomb engineering [75–77]. With a similar Hamiltonian to that of Eq. 7, we keep $t_{\alpha,\alpha+1}$ as a constant while U_α has the form

$$U(x_\alpha) = U_0 + U_1 \cos(k_1 x_\alpha) + U_2 \cos(k_2 x_\alpha), \quad (11)$$

as shown in Fig. 4 (a) and (b). We make use of the same k_1 and k_2 values applied in Eq. 9. For the results shown in Fig. 4 (c) and (d), we observe that at larger moiré scale the spectral functions are modified following k_2 while in the smaller moiré scale k_1 dominates the modulation. These results further validate the effectiveness of our approach in handling one-dimensional super-moiré systems with diverse and complex configurations.

Discussion—The methodology discussed above can be generalized to higher-dimensional systems, and long range-interactions can be included by writing the appropriate pseudo-spin many-body representations. Importantly, our approach relies on the compressibility of the single-particle and mean-field terms as tensor networks. While super-moiré systems are highly compressible due to the highly structured nature of the Hamiltonian, strongly disordered systems will have limited compressibility and thus will not be solvable with this technique. Crucially, our approach does not require storing the single particle Hamiltonian explicitly, and therefore allows one to tackle systems whose single-particle Hamiltonian is too large to be explicitly stored. This capability should be contrasted with previous Chebyshev self-consistent methods [56], which required storing the single-particle Hamiltonian as a sparse matrix. This vital difference allowed us to reach system sizes almost 1000 times bigger than those accessible by the previous methods [56]. The tensor-network representation of the mean-field Hamiltonian allows us to leverage traditional tensor network algorithms, including performing time evolution [78, 79], and can therefore be extended to compute real-space topological properties and quantum

transport in super-moiré materials. While our discussion has focused on tight-binding models, It is worth noting that our tensor-network mean-field methodology can be readily extended to real-space density functional theory [80–82], which can potentially enable an increase in the system sizes that these methods can reach.

Conclusion—In summary, we have established a methodology that allows us to solve billion-size interacting super-moiré problems by using a self-consistent tensor network algorithm. Our strategy uses a mapping from the real-space Hamiltonian of a system with a size of 2^L atomic sites into a tensor-network representation of a many-body system corresponding to a chain of L -site pseudo spins. By using a combination of tensor-network Chebyshev expansion and quantum tensor cross interpolation, we can solve the self-consistent mean-field equations of exponentially large systems. We demonstrate this technique with super-moiré interacting models above a billion sites, featuring a spatially-dependent single-particle term and spatially-dependent many-body interactions, including domain walls. Our work establishes a widely applicable technique to treat interacting electronic problems, providing a method to solve correlated systems of unprecedented sizes and in particular whose single-particle Hamiltonian alone is too large to be explicitly stored even with sparse representations. Ultimately, our work provides a starting point to perform many-body perturbation theory and linear response using tensor networks in real-space, providing the required method to rationalize a wide range of correlated phenomena in super-moiré quantum matter.

Acknowledgments—We acknowledge the computational resources provided by the Aalto Science-IT project and the financial support from Finnish Quantum Flagship, InstituteQ, QDOC, the Jane and Aatos Erkko Foundation and the Academy of Finland Projects Nos. 331342, 358088, and 349696. We thank X. Waintal, C. Flindt, C. Yu, P. San-Jose, E. Prada, B. Amorim and E. Castro for useful discussions. The code used in this work is available at [83].

-
- [1] J. M. Park, Y. Cao, K. Watanabe, T. Taniguchi, and P. Jarillo-Herrero, Tunable strongly coupled superconductivity in magic-angle twisted trilayer graphene, *Nature* **590**, 249255 (2021).
- [2] X. Lu, P. Stepanov, W. Yang, M. Xie, M. A. Aamir, I. Das, C. Urgell, K. Watanabe, T. Taniguchi, G. Zhang, A. Bachtold, A. H. MacDonald, and D. K. Efetov, Superconductors, orbital magnets and correlated states in magic-angle bilayer graphene, *Nature* **574**, 653657 (2019).
- [3] Y. Zhang, R. Polski, C. Lewandowski, A. Thomson, Y. Peng, Y. Choi, H. Kim, K. Watanabe, T. Taniguchi, J. Alicea, F. von Oppen, G. Refael, and S. Nadj-Perge, Promotion of superconductivity in magic-angle graphene multilayers, *Science* **377**, 15381543 (2022).
- [4] M. Yankowitz, S. Chen, H. Polshyn, Y. Zhang, K. Watanabe, T. Taniguchi, D. Graf, A. F. Young, and C. R. Dean, Tuning superconductivity in twisted bilayer graphene, *Science* **363**, 10591064 (2019).
- [5] A. Uri, S. C. de la Barrera, M. T. Randeria, D. Rodan-Legrain, T. Devakul, P. J. D. Crowley, N. Paul, K. Watanabe, T. Taniguchi, R. Lifshitz, L. Fu, R. C. Ashoori, and P. Jarillo-Herrero, Superconductivity and strong interactions in a tunable moiré quasicrystal, *Nature* **620**, 762767 (2023).
- [6] D. R. Klein, L.-Q. Xia, D. MacNeill, K. Watanabe, T. Taniguchi, and P. Jarillo-Herrero, Electrical switching of a bistable moiré superconductor, *Nature Nanotechnology* **18**, 331335 (2023).
- [7] Y. Zeng, Z. Xia, K. Kang, J. Zhu, P. Knüppel, C. Vaswani, K. Watanabe, T. Taniguchi, K. F. Mak, and J. Shan, Thermodynamic evidence of fractional chern insulator in moiré $m\text{ot}e_2$, *Nature* **622**, 6973 (2023).
- [8] J. Cai, E. Anderson, C. Wang, X. Zhang, X. Liu, W. Holtzmann, Y. Zhang, F. Fan, T. Taniguchi, K. Watanabe, Y. Ran, T. Cao, L. Fu, D. Xiao, W. Yao, and X. Xu, Signatures of fractional quantum anomalous hall states in twisted $m\text{ot}e_2$, *Nature* **622**, 6368 (2023).
- [9] M. Serlin, C. L. Tschirhart, H. Polshyn, Y. Zhang, J. Zhu, K. Watanabe, T. Taniguchi, L. Balents, and A. F. Young, Intrinsic quantized anomalous hall effect in a moiré heterostructure, *Science* **367**, 900903 (2020).
- [10] Z. Lu, T. Han, Y. Yao, A. P. Reddy, J. Yang, J. Seo, K. Watanabe, T. Taniguchi, L. Fu, and L. Ju, Fractional quantum anomalous hall effect in multilayer graphene, *Nature* **626**, 759764 (2024).
- [11] Y. Cao, V. Fatemi, A. Demir, S. Fang, S. L. Tomarken, J. Y. Luo, J. D. Sanchez-Yamagishi, K. Watanabe, T. Taniguchi, E. Kaxiras, R. C. Ashoori, and P. Jarillo-Herrero, Correlated insulator behaviour at half-filling in magic-angle graphene superlattices, *Nature* **556**, 8084 (2018).
- [12] W. Zhao, B. Shen, Z. Tao, Z. Han, K. Kang, K. Watanabe, T. Taniguchi, K. F. Mak, and J. Shan, Gate-tunable heavy fermions in a moiré kondo lattice, *Nature* **616**, 6165 (2023).
- [13] H. Kim, Y. Choi, L. Lantagne-Hurtubise, C. Lewandowski, A. Thomson, L. Kong, H. Zhou, E. Baum, Y. Zhang, L. Holleis, K. Watanabe, T. Taniguchi, A. F. Young, J. Alicea, and S. Nadj-Perge, Imaging inter-valley coherent order in magic-angle twisted trilayer graphene, *Nature* **623**, 942948 (2023).
- [14] V. Vao, M. Amini, S. C. Ganguli, G. Chen, J. L. Lado, S. Kezilebieke, and P. Liljeroth, Artificial heavy fermions in a van der waals heterostructure, *Nature* **599**, 582586 (2021).
- [15] E. Y. Andrei, D. K. Efetov, P. Jarillo-Herrero, A. H. MacDonald, K. F. Mak, T. Senthil, E. Tutuc, A. Yazdani, and A. F. Young, The marvels of moiré materials, *Nature Reviews Materials* **6**, 201206 (2021).
- [16] Q. Fu, P. Wang, C. Huang, Y. V. Kartashov, L. Torner, V. V. Konotop, and F. Ye, Optical soliton formation controlled by angle twisting in photonic moiré lattices, *Nature Photonics* **14**, 663668 (2020).
- [17] L. Du, M. R. Molas, Z. Huang, G. Zhang, F. Wang, and Z. Sun, Moiré photonics and optoelectronics, *Science* **379**, 10.1126/science.adg0014 (2023).
- [18] H. Tang, B. Lou, F. Du, M. Zhang, X. Ni, W. Xu,

- R. Jin, S. Fan, and E. Mazur, Experimental probe of twist angledependent band structure of on-chip optical bilayer photonic crystal, *Science Advances* **9**, 10.1126/sciadv.adh8498 (2023).
- [19] X.-R. Mao, Z.-K. Shao, H.-Y. Luan, S.-L. Wang, and R.-M. Ma, Magic-angle lasers in nanostructured moiré superlattice, *Nature Nanotechnology* **16**, 10991105 (2021).
- [20] A. A. Arkhipova, Y. V. Kartashov, S. K. Ivanov, S. A. Zhuravitskii, N. N. Skryabin, I. V. Dyakonov, A. A. Kalinkin, S. P. Kulik, V. O. Kompanets, S. V. Chekalin, F. Ye, V. V. Konotop, L. Torner, and V. N. Zadkov, Observation of linear and nonlinear light localization at the edges of moiré arrays, *Phys. Rev. Lett.* **130**, 083801 (2023).
- [21] Y. V. Kartashov, F. Ye, V. V. Konotop, and L. Torner, Multifrequency solitons in commensurate-incommensurate photonic moiré lattices, *Phys. Rev. Lett.* **127**, 163902 (2021).
- [22] H.-Y. Luan, Y.-H. Ouyang, Z.-W. Zhao, W.-Z. Mao, and R.-M. Ma, Reconfigurable moiré nanolaser arrays with phase synchronization, *Nature* **624**, 282288 (2023).
- [23] A. González-Tudela and J. I. Cirac, Cold atoms in twisted-bilayer optical potentials, *Phys. Rev. A* **100**, 053604 (2019).
- [24] T. Salamon, A. Celi, R. W. Chhajlany, I. Frérot, M. Lewenstein, L. Tarruell, and D. Rakshit, Simulating twistrionics without a twist, *Phys. Rev. Lett.* **125**, 030504 (2020).
- [25] J.-C. Yu, S. Bhave, L. Reeve, B. Song, and U. Schneider, Observing the two-dimensional bose glass in an optical quasicrystal, *Nature* **633**, 338343 (2024).
- [26] Z. Meng, L. Wang, W. Han, F. Liu, K. Wen, C. Gao, P. Wang, C. Chin, and J. Zhang, Atomic bose-einstein condensate in twisted-bilayer optical lattices, *Nature* **615**, 231236 (2023).
- [27] L. A. Gonzalez-Arraga, J. L. Lado, F. Guinea, and P. San-Jose, Electrically controllable magnetism in twisted bilayer graphene, *Phys. Rev. Lett.* **119**, 107201 (2017).
- [28] A. Ramires and J. L. Lado, Emulating heavy fermions in twisted trilayer graphene, *Phys. Rev. Lett.* **127**, 026401 (2021).
- [29] Y. Mao, D. Guerici, and C. Mora, Supermoiré low-energy effective theory of twisted trilayer graphene, *Phys. Rev. B* **107**, 125423 (2023).
- [30] S. Carr, S. Fang, and E. Kaxiras, Electronic-structure methods for twisted moiré layers, *Nature Reviews Materials* **5**, 748763 (2020).
- [31] Y. Li, M. Xue, H. Fan, C.-F. Gao, Y. Shi, Y. Liu, K. Watanabe, T. Taniuchi, Y. Zhao, F. Wu, X. Wang, Y. Shi, W. Guo, Z. Zhang, Z. Fei, and J. Li, Symmetry breaking and anomalous conductivity in a double-moiré superlattice, *Nano Letters* **22**, 62156222 (2022).
- [32] M. Kapfer, B. S. Jessen, M. E. Eisele, M. Fu, D. R. Danielsen, T. P. Darlington, S. L. Moore, N. R. Finney, A. Marchese, V. Hsieh, P. Majchrzak, Z. Jiang, D. Biswas, P. Dudin, J. Avila, K. Watanabe, T. Taniuchi, S. Ulstrup, P. Bggild, P. J. Schuck, D. N. Basov, J. Hone, and C. R. Dean, Programming twist angle and strain profiles in 2d materials, *Science* **381**, 677681 (2023).
- [33] S. R. White, Density matrix formulation for quantum renormalization groups, *Phys. Rev. Lett.* **69**, 2863 (1992).
- [34] U. Schollwöck, The density-matrix renormalization group, *Rev. Mod. Phys.* **77**, 259 (2005).
- [35] U. Schollwöck, The density-matrix renormalization group in the age of matrix product states, *Annals of Physics* **326**, 96192 (2011).
- [36] R. Ors, Tensor networks for complex quantum systems, *Nature Reviews Physics* **1**, 538550 (2019).
- [37] R. Dilip, Y.-J. Liu, A. Smith, and F. Pollmann, Data compression for quantum machine learning, *Phys. Rev. Res.* **4**, 043007 (2022).
- [38] Z.-Y. Han, J. Wang, H. Fan, L. Wang, and P. Zhang, Unsupervised generative modeling using matrix product states, *Phys. Rev. X* **8**, 031012 (2018).
- [39] E. Stoudenmire and D. J. Schwab, Supervised learning with tensor networks, in *Advances in Neural Information Processing Systems*, Vol. 29, edited by D. Lee, M. Sugiyama, U. Luxburg, I. Guyon, and R. Garnett (Curran Associates, Inc., 2016).
- [40] N. Nakatani and G. K.-L. Chan, Efficient tree tensor network states (ttns) for quantum chemistry: Generalizations of the density matrix renormalization group algorithm, *The Journal of Chemical Physics* **138** (2013).
- [41] G. K.-L. Chan, A. Keselman, N. Nakatani, Z. Li, and S. R. White, Matrix product operators, matrix product states, and ab initio density matrix renormalization group algorithms, *The Journal of Chemical Physics* **145** (2016).
- [42] S. Szalay, M. Pfeffer, V. Murg, G. Barcza, F. Verstraete, R. Schneider, and O. Legeza, Tensor product methods and entanglement optimization for ab initio quantum chemistry, *International Journal of Quantum Chemistry* **115**, 13421391 (2015).
- [43] M. Niedermeier, J. L. Lado, and C. Flindt, Simulating the quantum fourier transform, grover’s algorithm, and the quantum counting algorithm with limited entanglement using tensor networks, *Phys. Rev. Res.* **6**, 033325 (2024).
- [44] Y. Zhou, E. M. Stoudenmire, and X. Waintal, What limits the simulation of quantum computers?, *Phys. Rev. X* **10**, 041038 (2020).
- [45] C. Huang, F. Zhang, M. Newman, X. Ni, D. Ding, J. Cai, X. Gao, T. Wang, F. Wu, G. Zhang, H.-S. Ku, Z. Tian, J. Wu, H. Xu, H. Yu, B. Yuan, M. Szegedy, Y. Shi, H.-H. Zhao, C. Deng, and J. Chen, Efficient parallelization of tensor network contraction for simulating quantum computation, *Nature Computational Science* **1**, 578587 (2021).
- [46] F. Pastawski, B. Yoshida, D. Harlow, and J. Preskill, Holographic quantum error-correcting codes: toy models for the bulk/boundary correspondence, *Journal of High Energy Physics* **2015** (2015).
- [47] T. Farrelly, R. J. Harris, N. A. McMahon, and T. M. Stace, Tensor-network codes, *Phys. Rev. Lett.* **127**, 040507 (2021).
- [48] T. Farrelly, N. Milicevic, R. J. Harris, N. A. McMahon, and T. M. Stace, Parallel decoding of multiple logical qubits in tensor-network codes, *Phys. Rev. A* **105**, 052446 (2022).
- [49] Y. N. Fernández, M. K. Ritter, M. Jeannin, J.-W. Li, T. Kloss, T. Louvet, S. Terasaki, O. Parcollet, J. von Delft, H. Shinaoka, and X. Waintal, Learning tensor networks with tensor cross interpolation: new algorithms and libraries, [arXiv:2407.02454](https://arxiv.org/abs/2407.02454).
- [50] M. K. Ritter, Y. Núñez Fernández, M. Wallerberger, J. von Delft, H. Shinaoka, and X. Waintal, Quantics tensor cross interpolation for high-resolution parsimo-

- nious representations of multivariate functions, *Phys. Rev. Lett.* **132**, 056501 (2024).
- [51] H. Shinaoka, M. Wallerberger, Y. Murakami, K. Nogaki, R. Sakurai, P. Werner, and A. Kauch, Multiscale space-time ansatz for correlation functions of quantum systems based on quantum tensor trains, *Phys. Rev. X* **13**, 021015 (2023).
- [52] A. Erpenbeck, W.-T. Lin, T. Blommel, L. Zhang, S. Isakov, L. Bernheimer, Y. Núñez Fernández, G. Cohen, O. Parcollet, X. Waintal, and E. Gull, Tensor train continuous time solver for quantum impurity models, *Phys. Rev. B* **107**, 245135 (2023).
- [53] Y. Núñez Fernández, M. Jeannin, P. T. Dumitrescu, T. Kloss, J. Kaye, O. Parcollet, and X. Waintal, Learning feynman diagrams with tensor trains, *Phys. Rev. X* **12**, 041018 (2022).
- [54] H. Takahashi, R. Sakurai, and H. Shinaoka, Compactness of quantum tensor train representations of local imaginary-time propagators, *SciPost Phys.* **18**, 007 (2025).
- [55] M. Jeannin, Y. Núñez Fernández, T. Kloss, O. Parcollet, and X. Waintal, Cross-extrapolation reconstruction of low-rank functions and application to quantum many-body observables in the strong coupling regime, *Phys. Rev. B* **110**, 035124 (2024).
- [56] A. O. Fumega, M. Niedermeier, and J. L. Lado, Correlated states in super-moir materials with a kernel polynomial quantum tensor cross interpolation algorithm, *2D Materials* **12**, 015018 (2024).
- [57] M. Fishman, S. R. White, and E. M. Stoudenmire, The ITensor Software Library for Tensor Network Calculations, *SciPost Phys. Codebases*, 4 (2022).
- [58] [Quantics.jl](#).
- [59] M. Ritter and contributors, [Tensorcrossinterpolation.jl](#) (2022), email: Ritter.Marc@physik.uni-muenchen.de.
- [60] M. Ritter and contributors, [Quanticstci.jl](#) (2022), email: Ritter.Marc@physik.uni-muenchen.de.
- [61] A. Holzner, A. Weichselbaum, I. P. McCulloch, U. Schollwöck, and J. von Delft, Chebyshev matrix product state approach for spectral functions, *Phys. Rev. B* **83**, 195115 (2011).
- [62] J. L. Lado and O. Zilberberg, Topological spin excitations in harper-heisenberg spin chains, *Phys. Rev. Res.* **1**, 033009 (2019).
- [63] G. Chen, F. Song, and J. L. Lado, Topological spin excitations in non-hermitian spin chains with a generalized kernel polynomial algorithm, *Phys. Rev. Lett.* **130**, 100401 (2023).
- [64] G. Chen, J. L. Lado, and F. Song, Many-body liouvillian dynamics with a non-hermitian tensor-network kernel polynomial algorithm, *Phys. Rev. Res.* **6**, 043182 (2024).
- [65] A. Weiße, G. Wellein, A. Alvermann, and H. Fehske, The kernel polynomial method, *Rev. Mod. Phys.* **78**, 275 (2006).
- [66] The expansion in Eq. 5 can be formally applied with conventional sparse matrices H^{MF} , however, the full matrix with elements $\langle c_{\alpha}^{\dagger} c_{\beta} \rangle$ will be dense even when H^{MF} is sparse.
- [67] N. Jolly, Y. N. Fernandez, and X. Waintal, Tensorized orbitals for computational chemistry (2024), [arXiv:2308.03508](#).
- [68] I. Oseledets and E. Tyrtyshnikov, Tt-cross approximation for multidimensional arrays, *Linear Algebra and its Applications* **432**, 7088 (2010).
- [69] I. V. Oseledets, Tensor-train decomposition, *SIAM Journal on Scientific Computing* **33**, 22952317 (2011).
- [70] P. Wang, Y. Zheng, X. Chen, C. Huang, Y. V. Kartashov, L. Torner, V. V. Konotop, and F. Ye, Localization and delocalization of light in photonic moiré lattices, *Nature* **577**, 4246 (2019).
- [71] I. Caha, L. Boddapatti, A. ul Ahmad, M. Banobre, A. T. Costa, A. N. Enyashin, W. Li, P. Gargiani, M. Valvidares, J. Fernandez-Rossier, and F. L. Deepak, Magnetic single wall cri3 nanotubes encapsulated within multiwall carbon nanotubes (2024), [arXiv:2405.14967](#).
- [72] N. Nakatsuji, T. Kawakami, and M. Koshino, Multiscale lattice relaxation in general twisted trilayer graphenes, *Phys. Rev. X* **13**, 041007 (2023).
- [73] I. M. Craig, M. Van Winkle, C. Groschner, K. Zhang, N. Dowlatshahi, Z. Zhu, T. Taniguchi, K. Watanabe, S. M. Griffin, and D. K. Bediako, Local atomic stacking and symmetry in twisted graphene trilayers, *Nature Materials* **23**, 323330 (2024).
- [74] R. Engelke, H. Yoo, S. Carr, K. Xu, P. Cazeaux, R. Allen, A. M. Valdivia, M. Lusk, E. Kaxiras, M. Kim, J. H. Han, and P. Kim, Topological nature of dislocation networks in two-dimensional moiré materials, *Phys. Rev. B* **107**, 125413 (2023).
- [75] M. Rösner and J. L. Lado, Inducing a many-body topological state of matter through coulomb-engineered local interactions, *Phys. Rev. Res.* **3**, 013265 (2021).
- [76] Z. Jiang, S. Haas, and M. Rösner, Plasmonic waveguides from coulomb-engineered two-dimensional metals, *2D Materials* **8**, 035037 (2021).
- [77] T. Tan, A. P. Reddy, L. Fu, and T. Devakul, Designing topology and fractionalization in narrow gap semiconductor films via electrostatic engineering, *Phys. Rev. Lett.* **133**, 206601 (2024).
- [78] J. Haegeman, J. I. Cirac, T. J. Osborne, I. Pižorn, H. Verschelde, and F. Verstraete, Time-dependent variational principle for quantum lattices, *Phys. Rev. Lett.* **107**, 070601 (2011).
- [79] S. Paeckel, T. Köhler, A. Swoboda, S. R. Manmana, U. Schollwöck, and C. Hubig, Time-evolution methods for matrix-product states, *Annals of Physics* **411**, 167998 (2019).
- [80] J. Thijssen, *Computational physics* (Cambridge university press, 2007).
- [81] C. Pisani, R. Dovesi, and C. Roetti, *Hartree-Fock ab initio treatment of crystalline systems*, Vol. 48 (Springer Science & Business Media, 2012).
- [82] J. Enkovaara, C. Rostgaard, J. J. Mortensen, J. Chen, M. Duak, L. Ferrighi, J. Gavnholt, C. Glinsvad, V. Haikola, H. A. Hansen, H. H. Kristoffersen, M. Kuisma, A. H. Larsen, L. Lehtovaara, M. Ljungberg, O. Lopez-Acevedo, P. G. Moses, J. Ojanen, T. Olsen, V. Petzold, N. A. Romero, J. Stausholm-Miller, M. Strange, G. A. Tritsarlis, M. Vanin, M. Walter, B. Hammer, H. Häkkinen, G. K. H. Madsen, R. M. Nieminen, J. K. Nørskov, M. Puska, T. T. Rantala, J. Schitz, K. S. Thygesen, and K. W. Jacobsen, Electronic structure calculations with gpaw: a real-space implementation of the projector augmented-wave method, *Journal of Physics: Condensed Matter* **22**, 253202 (2010).
- [83] https://github.com/YITAOSUN42/SCF_with_MPO.